doi:10.1093/brain/awy099 BRAIN 2018: 141; 1840–1854 | 1840

BRAIN
A JOURNAL OF NEUROLOGY

Cognitive correlates of α4β2 nicotinic acetylcholine receptors in mild Alzheimer's dementia

Osama Sabri,[1,*] Philipp M. Meyer,[1,*] Susanne Gräf,[2,3] Swen Hesse,[1,4] Stephan Wilke,[1] Georg-Alexander Becker,[1] Michael Rullmann,[1,3,4] Marianne Patt,[1] Julia Luthardt,[1] Gudrun Wagenknecht,[5] Alexander Hoepping,[6] Rene Smits,[6] Annegret Franke,[7] Bernhard Sattler,[1] Solveig Tiepolt,[1] Steffen Fischer,[8] Winnie Deuther-Conrad,[8] Ulrich Hegerl,[2] Henryk Barthel,[1] Peter Schönknecht[2,*] and Peter Brust[8,*]

*These authors contributed equally to this work.

In early Alzheimer's dementia, there is a need for PET biomarkers of disease progression with close associations to cognitive dysfunction that may aid to predict further cognitive decline and neurodegeneration. Amyloid biomarkers are not suitable for that purpose. The α4β2 nicotinic acetylcholine receptors (α4β2-nAChRs) are widely abundant in the human brain. As neuromodulators they play an important role in cognitive functions such as attention, learning and memory. Post-mortem studies reported lower expression of α4β2-nAChRs in more advanced Alzheimer's dementia. However, there is ongoing controversy whether α4β2-nAChRs are reduced in early Alzheimer's dementia. Therefore, using the recently developed α4β2-nAChR-specific radioligand (−)-^{18}F-flubatine and PET, we aimed to quantify the α4β2-nAChR availability and its relationship to specific cognitive dysfunction in mild Alzheimer's dementia. Fourteen non-smoking patients with mild Alzheimer's dementia, drug-naïve for cholinesterase therapy, were compared with 15 non-smoking healthy controls matched for age, sex and education by applying (−)-^{18}F-flubatine PET together with a neuropsychological test battery. The one-tissue compartment model and Logan plot method with arterial input function were used for kinetic analysis to obtain the total distribution volume (V_T) as the primary, and the specific binding part of the distribution volume (V_S) as the secondary quantitative outcome measure of α4β2-nAChR availability. V_S was determined by using a pseudo-reference region. Correlations between V_T within relevant brain regions and Z-scores of five cognitive functions (episodic memory, executive function/working memory, attention, language, visuospatial function) were calculated. V_T (and V_S) were applied for between-group comparisons. Volume of interest and statistical parametric mapping analyses were carried out. Analyses revealed that in patients with mild Alzheimer's dementia compared to healthy controls, there was significantly lower V_T, especially within the hippocampus, fronto-temporal cortices, and basal forebrain, which was similar to comparisons of V_S. V_T decline in Alzheimer's dementia was associated with distinct domains of impaired cognitive functioning, especially episodic memory and executive function/working memory. Using (−)-^{18}F-flubatine PET in patients with mild Alzheimer's dementia, we show for the first time a cholinergic α4β2-nAChR deficiency mainly present within the basal forebrain-cortical and septohippocampal cholinergic projections and a relationship between lower α4β2-nAChR availability and impairment of distinct cognitive domains, notably episodic memory and executive function/working memory. This shows the potential of (−)-^{18}F-flubatine as PET biomarker of cholinergic α4β2-nAChR dysfunction and specific cognitive decline. Thus, if validated by longitudinal PET studies, (−)-^{18}F-flubatine might become a PET biomarker of progression of neurodegeneration in Alzheimer's dementia.

1 Department of Nuclear Medicine, University of Leipzig, Leipzig, Germany
2 Department of Psychiatry and Psychotherapy, University of Leipzig, Leipzig, Germany

Received November 3, 2017. Revised February 1, 2018. Accepted February 19, 2018. Advance Access publication April 17, 2018

3 Max-Planck-Institute for Human Cognitive and Brain Sciences, Leipzig, Germany
4 Integrated Research and Treatment Centre (IFB) Adiposity Diseases, University of Leipzig, Leipzig, Germany
5 Central Institute for Engineering, Electronics and Analytics—Electronic Systems (ZEA-2), Forschungszentrum Jülich, Jülich, Germany
6 ABX Advanced Biochemical Compounds GmbH, Radeberg, Germany
7 Centre for Clinical Trials Leipzig, University of Leipzig, Leipzig, Germany
8 Department of Neuroradiopharmaceuticals, Institute of Radiopharmaceutical Cancer Research, Helmholtz-Zentrum Dresden-Rossendorf, Research Site Leipzig, Leipzig, Germany

Correspondence to: Osama Sabri, MD, PhD
Department of Nuclear Medicine, University of Leipzig; Liebigstraße 18, 04103 Leipzig, Germany
E-mail: Osama.Sabri@medizin.uni-leipzig.de

Keywords: (−)-^{18}F-flubatine; PET; cognitive dysfunction; α4β2-nAChRs; Alzheimer's dementia

Abbreviations: α4β2-nAChR = α4β2 nicotinic acetylcholine receptor; GMD = grey-matter density; PVEC = partial volume effect correction; V_{ND} = non-displaceable distribution volume; V_S = specific binding part of the distribution volume; V_T = distribution volume

Introduction

Use of molecular imaging biomarkers such as amyloid-β PET significantly improves the clinical diagnosis of Alzheimer's dementia (McKhann *et al.*, 2011; Barthel *et al.*, 2015). However, amyloid-β PET is insufficient as surrogate marker for the prediction of neurodegenerative progression and cognitive deterioration. This is because a substantial number of elderly, apparently healthy subjects with significant amyloid-β plaque load do not develop frank dementia (Aizenstein *et al.*, 2008; Rowe *et al.*, 2010). Thus, there is a need for PET biomarkers of disease progression with close associations to cognitive dysfunction that may aid to predict further cognitive decline and neurodegeneration in mild Alzheimer's dementia (Teipel *et al.*, 2013).

According to the cholinergic hypothesis, there are deficiencies in the cholinergic pathways in Alzheimer's dementia which are associated with cognitive impairment (Francis *et al.*, 1999). In experimental Alzheimer's dementia, low levels of soluble amyloid-β inhibit cholinergic synaptic function even before significant amyloid-plaque loads occur (Klingner *et al.*, 2003; Lesné *et al.*, 2006; Schliebs and Arendt, 2011). The α4β2 nicotinic acetylcholine receptors (α4β2-AChRs) are widely expressed in the human brain, and decisively involved in cognitive functions such as attention, learning, and memory (Dani and Bertrand, 2007; Nees, 2015). Thus, PET imaging of cerebral α4β2-nAChRs might be sensitive to detect abnormalities early in the course of Alzheimer's dementia. In support of this assumption, post-mortem studies in patients with Alzheimer's dementia identified substantial decline in α4β2-nAChRs (Rinne *et al.*, 1991; Perry *et al.*, 1995). High-affinity α4β2-nAChR PET radioligands, such as 2-^{18}F-F-A85380, were developed to quantify α4β2-nAChR availability in the human brain *in vivo* (Kimes *et al.*, 2003). PET investigations in patients with Alzheimer's dementia and amnestic mild cognitive impairment, later converting to Alzheimer's dementia suggest that reductions of α4β2-nAChR availability are present early in the course of the disease and associated with cognitive dysfunction (Sabri *et al.*, 2008; Kendziorra *et al.*, 2011; Okada *et al.*, 2013). In contrast, other PET/SPECT studies did not find any significant differences of α4β2-nAChR availability between mild Alzheimer's dementia and healthy controls or relationships to cognitive dysfunction (Ellis *et al.*, 2008; Mitsis *et al.*, 2009*b*). This has led to the ongoing controversy regarding the questions, whether there is a decrease of α4β2-nAChR availability in mild Alzheimer's dementia and whether this decrease is related to cognitive decline. The relatively slow kinetics of 2-^{18}F-F-A85380 requiring acquisition times up to 7 h for full kinetic modelling, limits its use for clinical applications (Sabri *et al.*, 2008). Recently, a new generation of α4β2-nAChR-specific PET radioligands, such as (−)-^{18}F-flubatine, or ^{18}F-AZAN and ^{18}F-nifene, has been developed, showing high specific binding combined with fast kinetics (Brust *et al.*, 2008; Hillmer *et al.*, 2011; Wong *et al.*, 2013). We have previously published the pharmacokinetic modelling results of (−)-^{18}F-flubatine PET in healthy male subjects and identified favourable characteristics, i.e. (i) high brain uptake; (ii) fast kinetics; (iii) high stability; (iv) ability to describe α4β2-nAChR binding by a simple one-tissue-compartment model within 90 min for all regions of interest; and (v) proven safety and tolerability (Sattler *et al.*, 2014; Sabri *et al.*, 2015). In the current PET study, (−)-^{18}F-Flubatine has been applied in patients with Alzheimer's dementia in order to quantify alterations of α4β2-nAChRs. We hypothesize that (i) in mild Alzheimer's dementia compared with healthy controls, α4β2-nAChR availability is lower in distinct areas of the brain, especially those involving the fronto-temporo-parietal cortices and basal forebrain; and (ii) in Alzheimer's dementia, there is a relationship between α4β2-nAChR availability and domain-specific cognitive performance.

Materials and methods

This is a proof-of-concept, first-in-human study of prospectively recruited patients with Alzheimer's dementia and healthy, elderly controls, using the recently developed radioligand (−)-^{18}F-flubatine to investigate the α4β2-nAChR availability. In the previously published first part of this PET study, the

kinetic modelling characteristics of (−)-^{18}F-flubatine have been described (Sabri *et al.*, 2015).

Cohorts

Fourteen patients with mean (range) age 75.1 (58–83) years, with mild Alzheimer's dementia from the Department of Psychiatry, University Hospital Leipzig were compared with 15 healthy control subjects with mean (range) age 71.3 (63–77) years. To avoid possible effects not related to disease pathophysiology, patients with Alzheimer's dementia and healthy controls were matched for age, sex and education (Meyer *et al.*, 2009; Mitsis *et al.*, 2009*a*; Garibotto *et al.*, 2013). To achieve this patients and healthy controls were derived from a larger, unmatched study population ($n = 41$). All study subjects were non-smokers, drug-naïve for cholinesterase inhibitors, drug-free for any kind of centrally acting medication and had no history of neurological or psychiatric disorder other than Alzheimer's dementia. The diagnosis of mild, probable Alzheimer's dementia was made according to the NINCDS-ADRDA criteria characterized by progressive cognitive decline (in accordance with DSM-IV criteria for dementia), and a score of 1 on the Clinical Dementia Rating scale (CDR) and 24.0 ± 2.6 mean ± standard deviation (SD) on the Mini-Mental State Examination (MMSE). Healthy controls (CDR = 0) were recruited by newspaper advertisement and were required to achieve psychometric test results within 1 SD of the mean of reference normative data as provided by standard test manuals.

All subjects and patients gave written informed consent. The study was performed according to the 1964 Declaration of Helsinki and subsequent revisions, and was approved by the local ethics committee and the other competent authorities in Germany.

Neuropsychological assessment

This neuropsychological assessment included the full CERAD-Plus test battery (Category fluency, Letter fluency, Boston Naming Test, MMSE, Wordlist immediate and delayed recall; Wordlist savings score; Trail Making Test A and B), the subtests Logical Memory and Digit Span from the revised Wechsler Memory Scale, the Alters-Konzentrations-Test (AKT-G; a standardized geriatric cancellation test measuring attention/concentration), the Clock Drawing Test, the Multiple-Choice Vocabulary Intelligence Test (Morris *et al.*, 1989; Sunderland *et al.*, 1989; Härting *et al.*, 2000; Lehrl, 2005; Gatterer, 2008), and the Geriatric Depression Scale (GDS; Yesavage *et al.*, 1982-1983). Raw scores were converted to Z-scores by means of the normative data provided in the corresponding test manuals. Z-scores of relevant subtests were averaged to calculate five cognitive domains of interest, that are attention (AKT-G, digit span forward); executive function/working memory (Trail-Making-Test-B/A, letter fluency, digit span backward); visuospatial abilities (CERAD: visuoconstruction copy and recall), language (Boston Naming Test, category fluency); and episodic memory (CERAD: wordlist immediate and delayed recall, wordlist savings, visuoconstruction savings; WMS-R: Logical Memory immediate and delayed recall).

PET imaging procedures, kinetic modelling and analysis

(−)-^{18}F-flubatine was synthesized according to a recently published fully automated and good manufacturing practice compliant procedure (Patt *et al.*, 2013). The specific activity of (−)-^{18}F-flubatine was ∼1500 GBq/μmol at the time of injection (Patt *et al.*, 2013). PET data were obtained in 3D scanning mode with an ECAT Exact HR + system [Siemens/CTI, 63 slices, resolution 4.7 mm full-width at half-maximum (FWHM)] after the injection 90 s continuous short infusion (10 ml solution) of a dose of ∼370 MBq (−)-^{18}F-flubatine. Emission measurements consisted of one dynamic PET scan of 90 min (23 frames) and three subsequent scans (30 min, six frames each) starting at 2, 3 and 4 h post-injection, resulting in a total acquisition time of 270 min. Between the PET scans, starting after the first 90 min, patients and healthy controls were allowed to leave the PET system. PET data were corrected for scatter, attenuation (as estimated by means of a 10-min transmission scan acquired with three rotating ^{68}Ge rod sources before the first emission scan), and radioactive decay, and reconstructed by ordered subset expectation maximization with 10 iterations and 16 subsets with a pixel size of 0.2574 × 0.2574 × 0.2425 cm. PET and blood data processing were performed as recently described in detail. In the current data analysis only 0 to 90 min dynamic data were used since kinetic data analysis has shown that analysis of 0 to 90 min dynamic data allows accurate quantification of all brain regions (Patt *et al.*, 2014; Sabri *et al.*, 2015). In brief, tissue time activity curves from 0 to 90 min were used for kinetic analysis with a one-tissue compartment model to calculate the total distribution volume (V_T). For SPM analysis we needed a voxel-based approach to compute the distribution volume V_T. Thus, Logan's graphical analysis was applied on a voxel-wise basis to compute parametric images of V_T. Approximately 35 arterial plasma samples were obtained per subject to create individual input functions for kinetic modelling. Metabolite analysis showed high stability *in vivo* with 90% untransformed parent compound at 90 min. Because of the low number of metabolites (Sabri *et al.*, 2015) and to avoid errors introduced by the metabolite correction, the results presented were computed without metabolite correction. As recently reported, the plasma protein binding was 15 ± 2% and did not differ significantly between patients with Alzheimer's dementia and healthy controls (Patt *et al.*, 2014). K_1 is the delivery rate constant and equals the product of blood flow and extraction fraction of the radiotracer. As the extraction fraction is high for this tracer (Sabri *et al.*, 2015), K_1 was used as brain blood flow surrogate and indirect measure of neurodegeneration. K_1 values were computed from the PET data within a composite volume of interest, comprising the frontal, temporal, and parietal cortices, regions typically affected in Alzheimer's dementia.

It could be possible that the specific binding portion of the distribution volume (V_S)—not contaminated by non-displaceable binding—is more appropriate as receptor parameter for group comparisons between patients with Alzheimer's dementia and healthy controls. To account for interindividual variability in the non-displaceable distribution volume (V_{ND}), V_S was calculated using the corpus callosum as part of the white matter as pseudo-reference region, assuming that $V_T$corpus

callosum equals V_{ND} in all brain regions, as follows: $V_S = V_T$target region $- V_T$corpus callosum. Since the corpus callosum is the region of the brain with lowest V_T and mostly devoid of α4β2-nAChRs (Brody *et al.*, 2006), it was used as pseudo-reference region as published previously by α4β2-nAChR PET using 2-^{18}F-F-A85380 (Sabri *et al.*, 2008; Meyer *et al.*, 2009; Kendziorra *et al.*, 2011; Okada *et al.*, 2013). The use of the corpus callosum as pseudo-reference region for between-group comparisons was justified, because V_T within the corpus callosum in Alzheimer's dementia and healthy controls was similar and did not differ significantly. To account for morphometric changes that are present in Alzheimer's dementia and elderly healthy controls (Pini *et al.*, 2016) and which may affect the individual volume of interest analysis of the V_T data, additional approaches were carried out: the individual volumes of interest used to assess V_T were accounted for true grey matter density (GMD) as assessed by voxel-based analysis of MRI. Thus, GMD mask-weighted V_T values (V_TGMDW) were determined. Further, a partial volume effect (PVE) correction on the dynamic PET data, i.e. separately on each acquired time frame, was applied. For that purpose, we used the region-based voxel-wise (RBV) method as previously proposed and implemented (Thomas *et al.*, 2011, 2016). The PVE-corrected tissue time activity curves from 0–90 min were used for kinetic analysis with a one-tissue compartment model to calculate the PVE-corrected total distribution volume V_TPVEC.

MRI procedures and analysis

Subjects received 3 T brain MRI (Magnetom Trio, Siemens Healthcare) mainly to preclude relevant pathological findings not related to Alzheimer's dementia, and to determine the degree of medial temporal lobe atrophy and the extent of white matter lesions based on either the Scheltens or Fazekas Scale (Fazekas *et al.*, 1987; Scheltens *et al.*, 1992). The imaging protocol included a T_1-weighted magnetization prepared rapid gradient echo 3D sequence (MPRAGE; repetition time = 2130 ms, echo time = 3.03 ms, inversion time = 1200 ms, matrix 256 × 256 × 256, pixel bandwidth 130 Hz) and a transverse T_2-weighted turbo spin echo sequence. The MRI data were preprocessed using the VBM8 toolbox (http://dbm.neuro.uni-jena.de/vbm/download/) for SPM8 (Wellcome Trust Centre for Neuroimaging, UCL, London, UK) and MATLAB 7.13 (The MathWorks Inc., Natick, MA, USA). The default settings were used while correcting for bias-field inhomogeneity and generating the tissue probability maps for white and grey matter. Non-linear normalization was carried out using the Diffeomorphic Anatomical Registration Through Exponentiated Lie Algebra (DARTEL) approach (Ashburner, 2007). The resulting modulated (corrected for individual brain size) and spatially normalized data were smoothed using an 8 mm FWHM Gaussian kernel.

To denote the modulated and normalized grey matter probability values, the GMD was used. Forebrain analysis of GMD and V_T in the basal forebrain was carried out by extracting a binary mask of the basal forebrain cholinergic system (Ch1-3, Ch4) provided by the Anatomy Toolbox in SPM (Eickhoff *et al.*, 2005; Zaborszky *et al.*, 2008). The averaged GMD and averaged V_T inside the mask were calculated. Within the model, we masked the GMD maps by a threshold of 0.1 (absolute thresholding). Values of GMD as assessed by VBM within the hippocampus and basal forebrain in Alzheimer's dementia were compared with healthy controls.

Volume of interest and SPM analysis of PET data

The individual MRI datasets of patients and healthy subjects were spatially reoriented onto a standard brain dataset similar to Talairach space. For volume of interest analysis, cortical, subcortical, white matter and cerebellar regions of interest, except basal forebrain, were manually drawn bilaterally on three consecutive transversal slices (if necessary two or four slices) of the reoriented T_1-weighted-MPRAGE datasets using PMOD software (PMOD Technologies). The thickness of the MRI slices was transformed to 2.5 mm to enlarge the volume encompassed by the chosen consecutive slices as described previously in detail (Sabri *et al.*, 2015). The localizations of individually drawn regions of interest for the volume of interest analysis of the PET data are exemplified in the MRI of one study subject (Supplementary material and Supplementary Fig. 1). Voxel-based analysis was performed using SPM8. V_T maps were spatially normalized onto the individual 3D T_1 MPRAGE MRI and smoothed with 8 mm FWHM on a Gaussian filter.

Statistical analyses

Because this is a first-in-human PET investigation in Alzheimer's dementia using the recently developed radioligand (−)-^{18}F-flubatine and thus because of the paucity of data and the relatively small number of study cohorts, this study is exploratory in nature. Statistical analyses were performed with IBM SPSS statistic software, version 24. All variables were tested for normal distribution using the Kolmogorov-Smirnov test. For group comparisons of clinical and cognitive data of Alzheimer's dementia and healthy controls, two-tailed *t*-tests were performed (significance at $P < 0.05$). For group comparisons and correlation analyses regarding the volume of interest-based PET and MRI data, significance was regarded as relevant following correction for multiple testing using the false discovery rate (FDR) correction method ($P < 0.05_{corrected}$; Benjamini and Hochberg, 1995). For volume of interest analyses of PET data, the right and left side of the brain were pooled after ruling out significantly relevant right/left asymmetries (paired *t*-test; significance at $P < 0.05_{corrected}$). Group comparisons (Alzheimer's dementia versus healthy controls) of PET and MRI data were carried out applying ANCOVA (adjusted for age and sex). For volume of interest analysis, five brain regions with known Alzheimer's dementia pathology were selected *a priori*, such as the mean cortex (i.e. the frontal, lateral temporal, mesial temporal and parietal cortices), the basal forebrain, the frontal, mesial temporal (hippocampus), and parietal cortices (significance at $P < 0.05_{corrected}$; Kendziorra *et al.*, 2011; Barthel *et al.*, 2015). For *post hoc* volume of interest analysis of—at most—12 additional brain regions, a $P < 0.004_{uncorrected}$ ($P < 0.05_{corrected}$) was accepted as significant. For *post hoc*, exploratory SPM analysis of V_T parametric images, differences were accepted as significant at $P < 0.001_{uncorrected}$, extent threshold k = 5 voxels. Following correction for multiple

comparisons, $P < 0.05$ [family-wise error (FWE)-, FDR-, or set level-corrected] was considered as highly significant (Friston *et al.*, 1996; Buchert *et al.*, 2004; Meyer *et al.*, 2009).

To determine whether there were age-, sex-, or education-related effects on α4β2-nAChR availability within each cohort (healthy controls or Alzheimer's dementia), volume of interest-based analyses of V_T (or V_S) between study cohorts regarding sex were carried out using an unpaired two-tailed *t*-test (significance at $P < 0.002_{uncorrected}$; $P < 0.05_{corrected}$). Correlation analyses between V_T (or V_S) and education or age in each study cohort were performed using one-sided Pearson's correlation test (significance at $P < 0.002_{uncorrected}$; $P < 0.05_{corrected}$).

Volume of interest-based correlation analyses between PET data in distinct cortical volumes of interest and neuropsychological Z-scores characterizing the five cognitive partial functions (episodic memory, executive function/working memory, attention, language, and visuospatial abilities) were carried out in the Alzheimer's dementia cohort only, using partial correlation analysis (adjusted for education and sex). Significance was accepted at $P < 0.05_{corrected}$. According to review data from the literature, brain regions that are considered to be most relevant for each of the five cognitive domains, were identified as *a priori* selected volumes of interest. *A priori* selected volumes of interest were as follows: episodic memory (frontal, mesial temporal, parietal cortices and basal forebrain), executive function/working memory (frontal and parietal cortices), language (frontal and temporal cortices), attention (frontal and parietal cortices), and visuospatial function (parietal and occipital cortices; Cabeza and Nyberg, 2000; Foxe *et al.*, 2016). To explore correlations between episodic memory and PET data within subregions of the mesial temporal cortex, *post hoc* volume of interest-based correlation analysis between episodic memory and α4β2-nAChR availability within hippocampus and amygdala was carried out.

Post hoc, exploratory, voxel-based correlation analyses between parametric images of V_T and the five cognitive domains (Z-scores) in Alzheimer's dementia were performed, and an exploratory $P < 0.001_{uncorrected}$, extent threshold of $k = 5$ voxels was considered significant. Clusters surviving FWE, FDR, or set-level-correction at $P < 0.05$ were accepted as highly significant (Friston *et al.*, 1996; Buchert *et al.*, 2004; Meyer *et al.*, 2009).

Results

Study subjects

Patients with Alzheimer's dementia and healthy controls did not differ significantly from each other in education (13.1 ± 2.2 versus 13.8 ± 1.5 years; $P = 0.378$), age (75.1 ± 6.2 versus 71.3 ± 4.7 years; $P = 0.071$), and sex distribution (Alzheimer's dementia: four males/10 females, healthy controls: eight males/seven females; $P = 0.264$). MMSE was significantly lower in Alzheimer's dementia compared with healthy controls (24.0 ± 2.6 versus 28.4 ± 0.9, $P < 0.001$). Patients with Alzheimer's dementia, compared with healthy controls, had significantly higher GDS scores (7.4 ± 3.6 versus 3.3 ± 2.2, $P < 0.001$) indicating mild depressive symptoms. In Alzheimer's dementia, compared with healthy controls, Scheltens scores were significantly higher (1.4 ± 1.0 versus 0.7 ± 0.5, $P = 0.025$) implying atrophic, hippocampal changes. In Alzheimer's dementia, compared with healthy controls, in both cohorts, Fazekas scores were mildly increased, indicating mild white matter hyperintensities and thus mild small vessel disease. In Alzheimer's dementia, compared with healthy controls, there was a trend for higher Fazekas scores, without reaching significance (deep white matter hyperintensities: 1.3 ± 0.7 versus 0.8 ± 0.6, $P = 0.053$; periventricular white matter hyperintensities: 1.3 ± 0.8 versus 0.8 ± 0.7, $P = 0.074$) (Supplementary material and Supplementary Table 1). Compared with healthy controls, patients with Alzheimer's dementia showed significantly lower Z-scores in most cognitive tests, derived from the cognitive test battery, resulting in significantly lower Z-scores in four out of the five cognitive domains. Z-scores were mostly reduced in Alzheimer's dementia regarding visuospatial function and episodic memory followed by language and executive function/working memory ($P < 0.001$). The Z-score of attention did not significantly differ between Alzheimer's dementia and healthy controls ($P = 0.161$) (Table 1 and Supplementary Table 2).

Image data of neurodegeneration

Kinetic modelling of the PET data indicated in Alzheimer's dementia, compared with healthy controls, significantly lower K_1 values within the composite volume of interest of the fronto-temporo-parietal cortices (0.31 ± 0.04 versus 0.35 ± 0.04; −11%; $P = 0.006$; $P < 0.05_{corrected}$). VBM analysis revealed that in Alzheimer's dementia, compared with healthy controls, there was significantly lower grey-matter density in the hippocampus (right/left side pooled; 0.54 ± 0.11 versus 0.66 ± 0.06; −18%; $P < 0.001$; $P < 0.05_{corrected}$) and basal forebrain (0.29 ± 0.05 versus 0.36 ± 0.03; −19%; $P < 0.001$; $P < 0.05_{corrected}$).

Asymmetry of α4β2-nAChR availability within the brain

Following correction for multiple comparisons, no significant asymmetric differences within the brain of Alzheimer's dementia or healthy controls for any quantitative PET parameters of α4β2-nAChR availability were found.

Effect of education, sex and age on α4β2-nAChR availability

Following correction for multiple comparisons, in both cohorts there were no significant correlations between education or age and V_T (or V_S) within any of the 18 brain regions that were studied. Furthermore, no sex-related differences of V_T (or V_S) were found.

Table 1 Impaired cognitive domains in patients with Alzheimer's dementia compared with healthy controls

	Z-scores[a]			
	Alzheimer's dementia	Healthy controls	t/F	*P*-value
Attention[b]	0.31 (1.04)	0.78 (0.63)	−1.45	0.161
Executive function/working memory	−0.51 (0.89)	0.44 (0.80)	−3.02	**<0.001**
Language	−1.09 (1.00)	0.59 (0.51)	−5.75	**<0.001**
Visuospatial abilities	−2.05 (1.11)	−0.19 (0.82)	−5.13	**<0.001**
Episodic memory	−1.76 (0.80)	0.32 (0.70)	−7.51	**<0.001**

Degrees of freedom = 27.
[a]Z-scores are given as mean and standard deviation (in parentheses).
[b]ANCOVA was calculated for this variable to account for years of education as covariate.
Unpaired two-tailed *t*-test for the comparison between Alzheimer's dementia and healthy controls; significance at $P < 0.05$ (bold).

α4β2-nAChR availability in Alzheimer's dementia and healthy controls

Parametric images of the V_T exemplify typical regional α4β2-nAChR availability within the brain of one representative patient with Alzheimer's dementia and one healthy control subject, i.e. high within the thalamus, moderate within the striatum, brainstem, cerebellum and white matter centrum semiovale, low within the neocortex and limbic regions and very low within the corpus callosum. Compared to the healthy control subject, lower cortical, subcortical and cerebellar V_T in the patient with Alzheimer's dementia can be visualized (Fig. 1). ANCOVA of volume of interest data revealed that in Alzheimer's dementia, there was significantly lower V_T in four of the five *a priori* selected brain regions reaching significance within the composite volume of interest including fronto-temporo-parietal cortices (mean cortex; −5%; $P = 0.015$; $P < 0.05_{corrected}$), within the frontal cortex (−5%; $P = 0.020$; $P < 0.05_{corrected}$), hippocampus as part of the mesial temporal cortex (−10%; $P = 0.001$; $P < 0.05_{corrected}$), and basal forebrain (−10%; $P = 0.003$; $P < 0.05_{corrected}$; Table 2). For exploratory *post hoc* analyses, in Alzheimer's dementia, there was significantly lower V_T within the right anterior cingulate cortex (−3%; $P = 0.028$; $P < 0.05_{uncorrected}$), thalamus (−9%; $P = 0.011$; $P < 0.05_{uncorrected}$), pons/midbrain (−7%; $P = 0.027$; $P < 0.05_{uncorrected}$), cerebellar cortex (−6%; $P = 0.031$; $P < 0.05_{uncorrected}$), and white matter centrum semiovale (−1%; $P = 0.021$; $P < 0.05_{uncorrected}$), although none of those *post hoc* comparisons remained significant after correction for multiple comparisons.

Volume of interest analysis of V_S data revealed very similar findings as obtained by analysis of V_T. In Alzheimer's dementia, there was widespread lower V_S reaching significance within four of the five *a priori* selected brain regions such as the mean cortex (−14%, $P = 0.009$, $P < 0.05_{corrected}$), frontal cortex (−13%, $P = 0.016$, $P < 0.05_{corrected}$), hippocampus as part of the mesial temporal cortex (−23%, $P = 0.002$, $P < 0.05_{corrected}$), and basal forebrain (−34%, $P = 0.019$, $P < 0.05_{corrected}$). For *post hoc* selected brain regions, V_S was significantly lower within the anterior cingulate cortex (−8%, $P = 0.039$; $P < 0.05_{uncorrected}$), within the thalamus (−12%, $P = 0.021$; $P < 0.05_{uncorrected}$) and the centrum semiovale in the white matter (−2%, $P = 0.030$; $P < 0.05_{uncorrected}$), although those *post hoc* findings for group comparisons did not remain significant after correction for multiple comparisons (Supplementary material and Supplementary Table 3).

Compared with healthy controls, in Alzheimer's dementia, there was significantly lower V_TGMDW and V_TPVEC within similar *a priori* selected cortical brain regions, as found by between-group comparisons for V_T and V_S measures. In contrast to V_T (and V_S) measures, however, for V_TGMDW and V_TPVEC, following correction for multiple comparisons, significance in those *a priori* regions was reached only within the hippocampus and basal forebrain. In Alzheimer's dementia, compared with healthy controls, per cent reductions of V_TGMDW were the lowest (Supplementary material, Supplementary Tables 4 and 5).

The explorative *post hoc* SPM analysis supported the findings from the volume of interest analyses, although significant clusters within the cortical brain regions typically affected by Alzheimer's dementia pathology were small. In Alzheimer's dementia, there were clusters with significantly lower V_T in the neocortex especially within the *a priori* defined brain regions such as the fronto-temporo-parietal cortices, the right hippocampus, and also within the cingulate cortex ($P < 0.001_{uncorrected}$; extent threshold k = 5 voxels; $P < 0.05_{set\text{-}level\ corrected}$; Fig. 2 and Table 3).

Relationship between α4β2-nAChR availability and cognition in Alzheimer's dementia

In patients with Alzheimer's dementia, the volume of interest-based correlation analyses revealed that there were significant positive associations between episodic memory and V_T within *a priori* defined brain regions such as the frontal (r = 0.78; $P = 0.004$), mesial temporal (r = 0.71; $P = 0.01$) and parietal cortices (r = 0.67; $P = 0.02$) (all $P < 0.05_{corrected}$; Table 4). There was no significant relationship between memory and

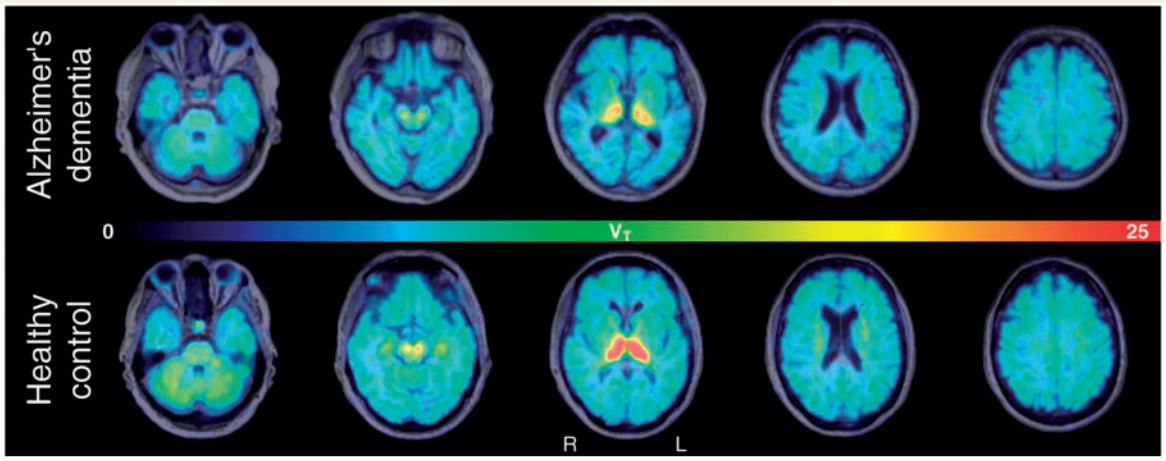

Figure 1 Parametric images of α4β2-nAChR availability (V_T) in a patient with Alzheimer's dementia and a healthy control subject. Parametric images of the V_T co-registered to individual MRI (transaxial views) exemplify the pattern of regionally distinct α4β2-nAChR availability in one representative patient with Alzheimer's dementia (*top*; male, aged 75 years, MMSE = 25, CDR = 1) and one healthy control subject (*bottom*; female, aged 71 years, MMSE = 28, CDR = 0). In the Alzheimer's dementia patient, compared with the healthy control subject, widespread decrease of α4β2-nAChR availability (V_T) within the cortex and thalamus was observed. As indicated by the pseudo-coloured bar, V_T values range from low (blue) to high (red).

Table 2 Reduced α4β2-nAChR availability (V_T) in Alzheimer's dementia compared with healthy controls using volume of interest analysis

V_T	Alzheimer's dementia (*n* = 14)		Healthy controls (*n* = 15)		Change of AD compared with HC (%)	*t*/*F*	*P*-value
	Mean	SD	Mean	SD			
Mean cortex[a]	8.69	1.00	9.18	0.53	−5	4.25	**0.015**
Frontal cortex[a]	8.77	1.09	9.26	0.62	−5	3.93	**0.020**
Lateral temporal cortex	8.61	0.98	8.95	0.46	−4	3.30	0.037
Mesial temporal cortex	8.59	1.07	9.37	0.59	−8	5.29	0.006
Hippocampus[a]	8.94	1.23	9.94	0.67	−10	7.62	**0.001**
Amygdala	9.13	1.21	9.60	0.82	−5	1.30	0.297
Parietal cortex[a]	8.79	1.07	9.14	0.65	−4	2.59	0.075
Occipital cortex	8.05	0.88	8.03	0.37	0	1.79	0.175
Basal forebrain[a]	7.29	1.48	8.08	1.02	−10	6.15	**0.003**
Anterior cingulate cortex	8.92	0.98	9.24	0.82	−3	3.58	0.028
Posterior cingulate cortex	9.07	0.98	9.27	0.69	−2	0.91	0.451
Caudate nucleus	9.96	1.29	10.22	0.82	−3	0.65	0.588
Putamen	11.51	1.38	11.40	0.81	1	0.66	0.588
Thalamus	23.11	3.37	25.46	3.16	−9	4.53	0.011
Pons/midbrain	10.35	1.23	11.13	0.87	−7	3.62	0.027
Cerebellar cortex	11.90	1.49	12.71	0.80	−6	3.48	0.031
Corpus callosum	5.81	0.83	5.85	0.59	−1	1.39	0.268
White matter centrum semiovale	10.01	1.53	10.11	1.09	−1	3.87	0.021

[a]*A priori* selected brain region with known Alzheimer's dementia pathology.
ANCOVA for the comparison of V_T between Alzheimer's dementia and healthy controls (adjusted for age and sex), within five *a priori* defined cortical brain regions, such as mean cortex, frontal, mesial temporal (hippocampus), parietal cortices, and basal forebrain (in bold); significance at $P < 0.05_{corrected}$ (FDR correction according to Benjamini-Hochberg; in bold). Furthermore, exploratory *post hoc* analysis for 12 additional brain regions, significance at $P < 0.004_{uncorrected}$ ($P < 0.05_{corrected}$; FDR correction).
AD = Alzheimer's dementia; HC = healthy controls.

V_T within the basal forebrain (r = 0.40; $P = 0.13$). Executive function/working memory and V_T showed significant positive associations within the frontal (r = 0.57; $P = 0.04$) and parietal cortices (r = 0.81; $P = 0.002$) (all $P < 0.05_{corrected}$; Table 4). There were no significant correlations between attention and V_T within the frontal and parietal cortices, between language and V_T within the frontal and temporal cortices, and between visuospatial function and V_T within the parietal and occipital cortices (Table 4).

Furthermore, exploratory, voxel-based correlation analyses identified significant positive correlations between memory dysfunction (Z-scores) and parametric images of reduced V_T

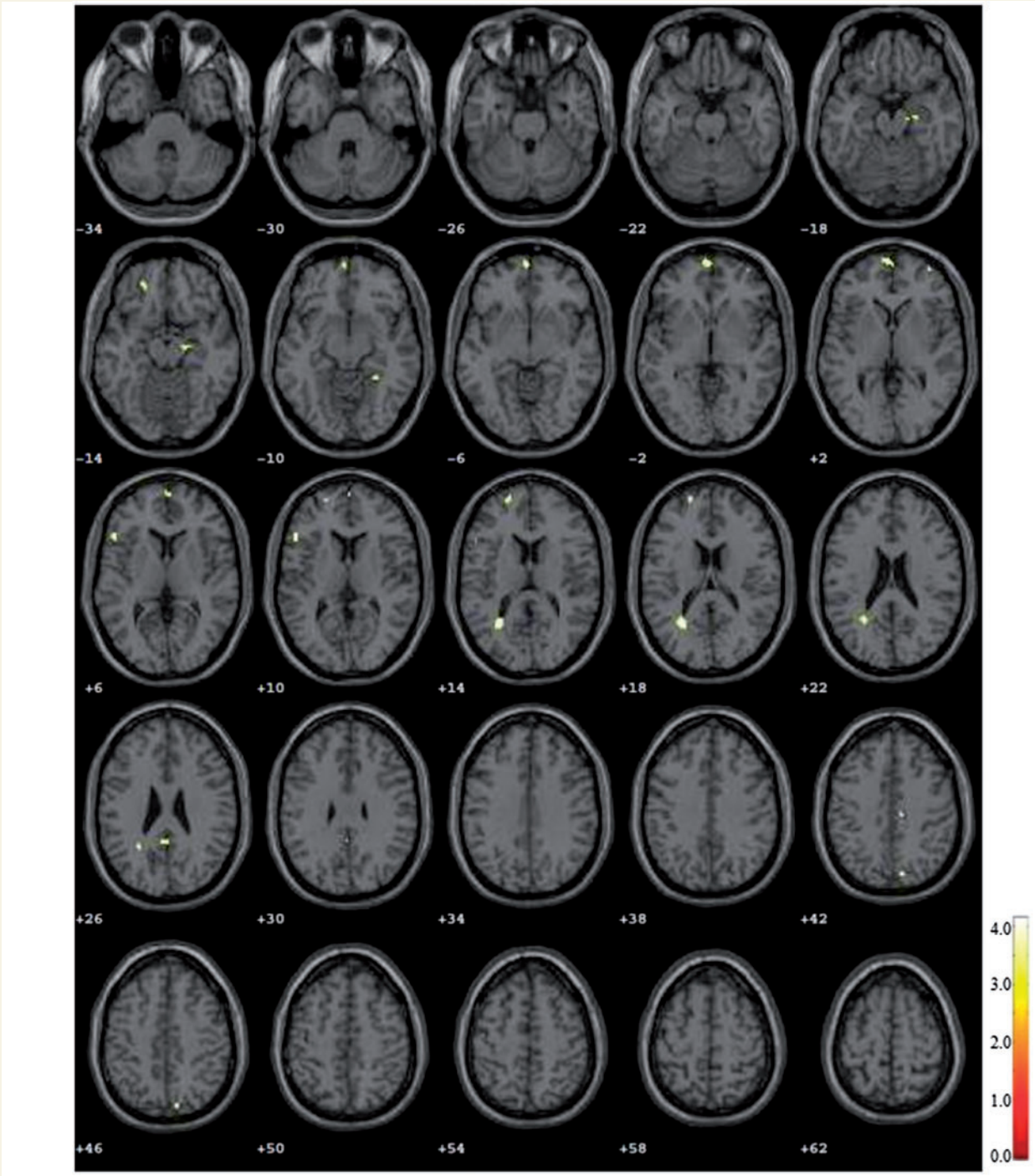

Figure 2 Reduced α4β2-nAChR availability (V_T) in Alzheimer's dementia compared with healthy controls using SPM analysis. Exploratory *post hoc* SPM analysis for the comparison of V_T parametric images in Alzheimer's dementia and healthy controls. Coloured clusters projected into transaxial slices of a standard MRI brain indicate significantly lower V_T in patients with Alzheimer's dementia compared with healthy controls, especially within the fronto-temporo-parieto cortices, and limbic regions (parahippocampus, posterior cingulate cortex). ANCOVA for group comparisons (adjusted for age and sex). Significance at $P < 0.001_{uncorrected}$; k = 5 voxels; $P < 0.05_{set\text{-}level\ corrected}$.

in Alzheimer's dementia, especially within the left basal forebrain and left inferior frontal cortex (cluster level: $P = 0.003_{uncorrected}$; $P < 0.05_{FWE\text{-}corrected}$), and furthermore, although not significant following correction for multiple comparisons, between the inferior temporal cortex, bilaterally, including the left parahippocampal gyrus (Fig. 3A and Table 5). There were significant, positive correlations between impaired executive function/working memory and lower V_T within the left inferior temporal, right superior temporal and right parietal cortices in Alzheimer's dementia (Fig. 3B and

Table 3 Lower α4β2-nAChR availability (V_T) in patients with Alzheimer's dementia compared with healthy controls using SPM analysis

SPM region[a], Alzheimer's dementia < healthy controls	Side of the brain	Cluster size[b]	Coordinates[c], mm (x, y, z)			T-score[d]	Z-score[e]	P-value, uncorrected[f]
Frontal lobe								
Frontal_Inf_Tri	L	37	−50	22	8	4.09	3.54	<0.0001
Frontal_Sup	L	28	−20	58	14	3.84	3.37	<0.0001
Frontal_Med_Orb	L	93	−2	64	−4	3.76	3.31	<0.0001
Frontal_Sup_Medial	R/L		2	64	8	3.65	3.24	0.001
Frontal_Sup_Orb	L	19	−22	44	−14	3.62	3.21	0.001
Frontal_Mid	R	8	38	58	0	3.56	3.17	0.001
Temporal lobe								
Fusiform, lingual	R	9	28	−44	−10	3.61	3.21	0.001
Limbic lobe								
Hippocampus	R	28	16	−14	−16	3.76	3.32	<0.0001
Parietal lobe								
Precuneus, calcarine	L	115	−28	−58	16	4.14	3.58	<0.0001
Occipital lobe								
Cuneus, precuneus	R	17	12	−76	42	3.81	3.35	<0.0001

[a]SPM regions of lower (−)-^{18}F-flubatine distribution volume (V_T) in patients with Alzheimer's dementia compared with healthy controls.
ANCOVA for the comparison between Alzheimer's dementia and healthy controls with age and sex as covariates.
[b]Cluster size is expressed in 2 mm^3 voxels.
[c]Location of the peak in the 3D stereotactic coordinates (*x*, *y*, *z*).
[d]Standardized *T*-scores.
[e]Standardized Z-scores.
[f]Significance was accepted at $P < 0.001_{uncorrected}$; extent threshold of k = 5 voxels, $P < 0.05_{set\text{-}level\ corrected}$, number of clusters = 13.
L = left; MNI = Montreal Neurological Institute; R = right; SPM = Statistical Parametric Mapping.

Table 4 Volume of inteerest-based correlation analysis between cortical α4β2-nAChR availability (V_T) within *a priori*-defined brain regions and five cognitive domains (Z-scores) in the Alzheimer's dementia cohort

Brain region		Basal forebrain df = 8	Frontal cortex df = 8	Mesial temporal cortex df = 8	Parietal cortex df = 8	Occipital cortex df = 8
Episodic memory[a]	r	0.40	**0.78**	**0.71**	**0.67**	n.a.
	P	0.128	0.004	0.010	0.018	n.a.
Executive function / WM[a]	r	n.a.	**0.57**	n.a.	**0.81**	n.a.
	P	n.a.	0.041	n.a.	0.002	n.a.
Attention[a]	r	n.a.	0.31	n.a.	0.41	n.a.
	P	n.a.	0.190	n.a.	0.117	n.a.
Language[a]	r	n.a.	0.02	0.25	n.a.	n.a.
	P	n.a.	0.477	0.245	n.a.	n.a.
Visuospatial function[a]	r	n.a.	n.a.	n.a.	0.22	0.25
	P	n.a.	n.a.	n.a.	0.272	0.245

[a]Partial correlations were calculated for this variable (corrected for education and sex).
[b]Bold coefficients represent significant correlations after controlling for multiple testing according to Benjamini-Hochberg ($P < 0.05_{corrected}$).
df = degrees of freedom; n.a. = not applicable; r = correlation coefficient; WM = working memory.

Table 5) ($P < 0.001_{uncorrected}$). There were significant, positive associations between impairment of attention and reduced V_T within the right frontal white matter, left thalamus, and left putamen in Alzheimer's dementia (Fig. 3C and Table 5) ($P < 0.001_{uncorrected}$). Significant, positive associations between language and V_T within the right cerebellum (crus 1 and 2) in Alzheimer's dementia were found (Table 5, $P < 0.001_{uncorrected}$). No significant positive correlations between V_T and visuospatial function were identified. There were no significant, negative correlations between any cognitive domains and V_T.

Post hoc volume of interest-based correlation analysis between episodic memory and PET data within subregions of the mesial temporal cortex showed a trend for a positive correlation within the hippocampus and a significant, positive correlation within the amygdala (Supplementary material). As compared to V_T, major findings for those correlations between cognition and additional PET

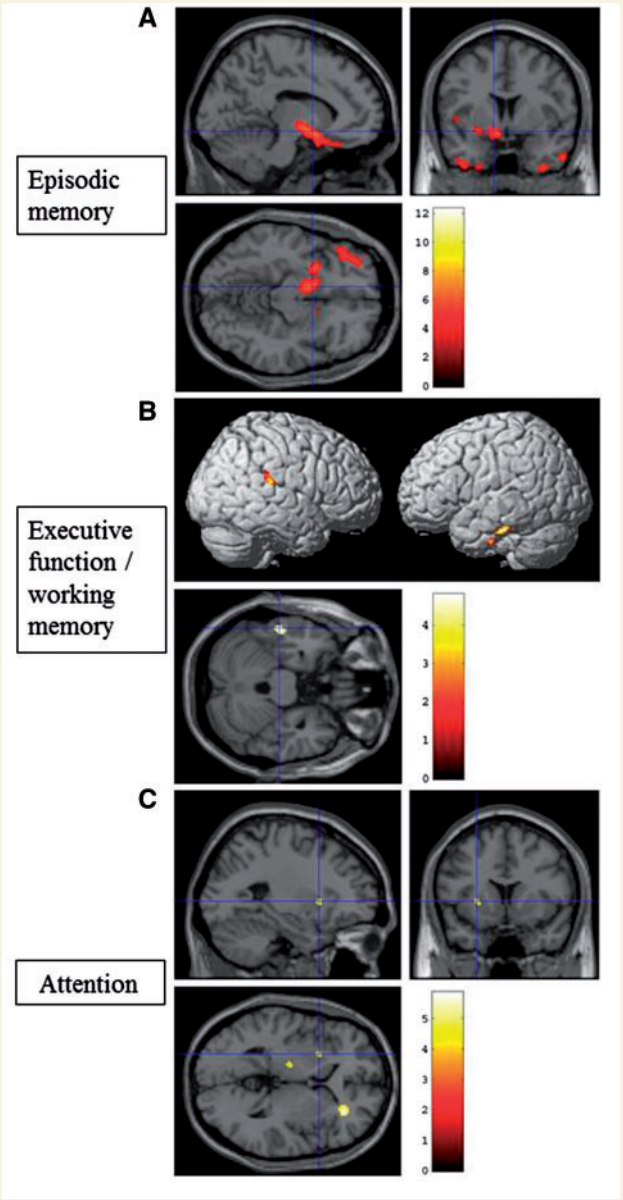

Figure 3 Cognitive correlates of lower α4β2-nAChR availability (V_T) in Alzheimer's dementia as assessed by SPM analysis. Exploratory, linear correlation analyses using SPM identify significant positive correlations between parametric images of V_T and impairment of various cognitive domains (Z-scores) in Alzheimer's dementia as projected into a standard MRI brain and indicated by coloured clusters (significance at $T > 3.93$; $P < 0.001_{uncorrected}$; k = 5 voxels). Memory dysfunction is positively correlated with V_T especially within the left basal forebrain and inferior frontal cortex (cluster-level: $P = 0.003_{uncorrected}$; $P < 0.05_{FWE\text{-}corrected}$) and inferior temporal cortex and parahippocampus (**A**). There is a positive relationship between altered executive function/working memory and V_T within the left inferior temporal, right superior temporal and right parietal cortices (**B**). Impairment of attention is positively associated with lower V_T within the right frontal white matter, left thalamus, and left putamen (**C**). No significant negative correlations were found.

parameters were similar, although the significance levels were lower (Supplementary material).

Discussion

Using novel (−)-^{18}F-flubatine and PET, the availability of α4β2-nAChRs in the brain of non-smoking, cholinergic drug-naïve patients with mild Alzheimer's dementia was quantitatively investigated and compared with healthy controls. This was accomplished to answer the question whether there is lower α4β2-nAChR availability early in the course of Alzheimer's dementia and whether this α4β2-nAChR state is related to cognitive decline (Sabri *et al.*, 2008; Kendziorra *et al.*, 2011; Okada *et al.*, 2013). PET analyses in Alzheimer's dementia reveal that there is a reduction of α4β2-nAChR availability in *a priori* defined multiple cortical brain regions as measured in absolute (V_T) and relative quantitative parameters (V_S). Regardless of the method used to quantify the α4β2-nAChR availability by kinetic modelling of PET data, brain regions typically affected by Alzheimer's dementia, such as the basal forebrain, hippocampus, and fronto-temporal cortices, demonstrate a deficiency. Regarding regional preferences of this deficiency, in Alzheimer's dementia, the α4β2-nAChR availability is mostly reduced in the hippocampus and basal forebrain, i.e. −10% and −10% in V_T and −23% and −34%, respectively, in V_S. As V_S is proportional to the receptor density, the reduction of V_S in Alzheimer's dementia is a direct measure of the reduction of the α4β2-nAChR density. The lower per cent reduction of V_T (as compared to V_S) reflects the additional non-displaceable distribution volume V_{ND} (i.e. $V_{ND} = V_T - V_S$), which is, as assessed by $V_T$corpus callosum, not different in Alzheimer's dementia and healthy controls (Innis *et al.*, 2007). As exploratory *post hoc* volume of interest analysis suggests, though not significant following correction for multiple testing, there may be also lower α4β2-nAChR availability within additional brain regions such as the pons, thalamus, and cerebellar cortex in mild Alzheimer's dementia. If these adjunct findings are verified in future PET studies, in mild Alzheimer's dementia, diminutions of cholinergic α4β2-nAChRs may not be restricted to the basal forebrain-cortical and septohippocampal cholinergic projections, but may be present also within the pontine-thalamic-cortical projection system, possibly representing dysfunction of non-cholinergic, e.g. noradrenergic systems, known to express α4β2-nAChRs (Dani and Bertrand, 2007; Theofilas *et al.*, 2017).

Our results strongly support and extend earlier PET/SPECT findings using first-generation, α4β2-nAChR-specific radioligands, such as 2-^{18}F-F-A85380 or 5-^{123}I-I-A85380. Those PET/SPECT studies detected lower α4β2-nAChR availability in mild-to-moderate Alzheimer's dementia only by relative quantitative measures (O'Brien *et al.*, 2007; Sabri *et al.*, 2008; Kendziorra *et al.*, 2011; Okada *et al.*, 2013). However, those results were not supported by other PET/SPECT imaging studies using the absolute quantitative

Table 5 Voxel-based correlation analyses demonstrate positive correlations between lower α4β2-nAChR availability (V_T) and dysfunction of episodic memory, executive function/working memory, attention and language in patients with Alzheimer's dementia

SPM region[a]		Side of the brain	Cluster size[b]	Coordinates[c], mm (x, y, z)			T-score[d]	Z-score[e]	P-value[f], uncorrected
Episodic memory									
Frontal lobe	Frontal_Inf_Orb[g]	L	1631	−20	18	−20	12.30	5.51	<0.0001
	Basal Forebrain[g]	L		−12	−4	−6	6.63	4.22	<0.0001
	Basal Forebrain[g]	L		−12	10	−12	6.53	4.19	<0.0001
	Rectus	R	184	12	16	−16	5.15	3.67	<0.0001
	Frontal_Sup_Orb	R		18	24	−22	5.12	3.66	<0.0001
	Rolandic_Oper	R	108	60	−10	10	5.04	3.62	<0.0001
	Rolandic_Oper	L	14	−48	4	2	4.12	3.19	0.001
Temporal lobe	Temporal_Inf	L	587	−54	−8	−34	7.71	4.55	<0.0001
	Temporal_Inf	L		−40	−2	−44	5.91	3.97	<0.0001
	Fusiform	L		−28	8	−44	5.13	3.66	<0.0001
	Temporal_Pole_Mid	R	132	38	10	−44	6.49	4.17	<0.0001
	Temporal_Inf	R	34	56	4	−34	4.70	3.47	<0.0001
	Temporal_Sup	R	108	52	−4	0	5.66	3.88	<0.0001
	Temporal_Inf	R	6	66	−14	−30	4.10	3.18	0.001
Limbic lobe	Parahippocampus	L	22	−18	−10	−28	4.29	3.28	0.001
	Parahippocampus	L		−24	−18	−28	4.01	3.13	0.001
Executive function/working memory									
Temporal lobe	Temporal_Inf	L	40	−54	−26	−26	4.79	3.52	<0.001
	Temporal_Inf	L	13	−44	−14	−36	4.41	3.34	<0.001
Parietal lobe	Supramarginal/temporal_Sup	R	35	54	−30	18	4.37	3.32	<0.001
Attention									
Frontal lobe	White matter	R	139	28	36	4	5.85	3.77	<0.0001
Striatum	Putamen	L	13	−26	12	2	4.57	3.28	0.001
Thalamus	Thalamus	L	8	−16	−16	2	4.43	3.22	0.001
Language									
Cerebellum	Lobule VII_Crus2	R	7	6	−84	−38	4.18	3.22	<0.001
	Lobule VII_Crus1	R	6	10	−82	−26	4.07	3.16	<0.001

[a]SPM regions of significant positive correlation between (−)-^{18}F-flubatine distribution volume (V_T) in patients with Alzheimer's dementia and episodic memory, executive function/working memory, attention and language (Z-scores). Linear correlation analysis in Alzheimer's dementia between V_T and distinct cognitive domains.
[b]Cluster size is expressed in 2 mm^3 voxels.
[c]Location of the peak in the stereotactic coordinates.
[d]Standardized *T*-scores.
[e]Standardized Z-scores.
[f]Significance was accepted at $P < 0.001_{uncorrected}$; extent threshold of k = 5 voxels.
[g]Brain region with significance following correction for multiple comparisons at $P = 0.003_{uncorrected}$, $P < 0.05_{FWE\text{-}corrected}$ (cluster-level).
L = left; R = right; SPM = Statistical Parametric Mapping.

measure V_T as outcome measure to assess α4β2-nAChR availability in mild Alzheimer's dementia, leading to an ongoing controversy (Ellis *et al.*, 2008; Mitsis *et al.*, 2009*b*). Conflicting results by prior PET/SPECT studies may not only be due to methodological differences how to quantify the α4β2-nAChR availability, but also due to clinical data variability, such as heterogeneity of dementia severity, presence of genetic risk factors, and differences in the age of onset of the disease.

In the present (−)-^{18}F-flubatine PET study, significantly lower α4β2-nAChR availability in Alzheimer's dementia was found, which ranges from −5 to −10% for V_T and −13 to −34% for V_S, differences that are smaller than expected from respective post-mortem studies (Rinne *et al.*, 1991; Perry *et al.*, 1995). These findings are less surprising since most of the Alzheimer's dementia patients investigated in our PET study have only mild dementia and 13 of 14 (93%) have the most common form of late onset-type Alzheimer's dementia. Moreover, the post-mortem studies used ^{3}H-nicotine, a radioligand that does not bind selectively to α4β2-nAChRs, as suggested by the presence of high- and low-affinity binding sites (Perry *et al.*, 1989). Of interest and similar to our findings regarding α4β2-nAChRs, modest diminutions of brain acetylcholinesterase, vesicular acetylcholine transporters and glucose metabolism using PET/SPECT in (mild) late-onset Alzheimer's dementia, were reported, mainly present within the temporal cortex (Kuhl *et al.*, 1996; Bohnen *et al.*, 2003; Kim *et al.*, 2005). These findings in late-onset Alzheimer's dementia were in contrast to more pronounced and widespread cortical defects in early-onset Alzheimer's dementia (Kuhl *et al.*, 1996; Kim *et al.*, 2005). The relatively small, mean

between-group differences of α4β2-nAChR availability might also be due to variance in both cohorts, reflecting normal, interindividual differences, ageing-related effects, and/or compensatory changes in early Alzheimer's dementia (Ellis *et al.*, 2008; Kantarci *et al.*, 2010). Of note, in mild Alzheimer's dementia, decrease of α4β2-nAChR availability is most pronounced in the mesial temporal cortex and basal forebrain where tau aggregations start (Yin, *et al.*, 2016). In this regard, recent experimental studies and a combined amyloid-β and α4β2-nAChR PET investigation in Alzheimer's dementia determined direct relationships between α4β2-nAChRs and tau or amyloid-β aggregations, hallmarks of Alzheimer's dementia pathology (Okada *et al.*, 2013; Ballinger *et al.*, 2016; Yin *et al.*, 2016). Future clinical PET association studies using radioligands to quantitatively assess tau and/or amyloid-β aggregations and α4β2-nAChR availability in Alzheimer's dementia will highly improve the understanding of α4β2-nAChR pathophysiology, and help to develop novel drug therapies (Okada *et al.*, 2013; Lombardo and Maskos, 2015; Kamkwalala and Newhouse, 2017). As compared to ^{18}F-FDG, which is currently used as clinical symptomatic disease PET biomarker of Alzheimer's dementia, and compared to tau PET tracers, which are currently tested in a similar regard, we see the potential advantage of (−)-^{18}F-flubatine PET by delivering specific information on the integrity of the cholinergic system, potentially simplifying 'go' or 'no-go' decisions on specific cholinergic treatment (Richter *et al.*, 2018). To investigate this feature, however, additional comparative PET tracer studies connected with clinical outcome readouts after treatment will be required.

Correlation analyses reveal that, in patients with Alzheimer's dementia, there is a strong relationship between impaired episodic memory and reduced α4β2-nAChR availability, especially within the fronto-temporo-parietal cortices and basal forebrain, such brain regions in which α4β2-nAChR diminutions are most pronounced in Alzheimer's dementia. The regional pattern of these associations, especially within the fronto-temporo-parietal cortices and basal forebrain, is in line with previous investigations (Cabeza and Nyberg, 2000). Thus, our PET findings strongly support and extend the cholinergic α4β2-nAChRs hypothesis for patients with mild Alzheimer's dementia, which has been challenged and revisited previously (Ellis *et al.*, 2008; Sabri *et al.*, 2008; Mitsis *et al.*, 2009*b*; Okada *et al.*, 2013; Ballinger *et al.*, 2016). To our knowledge, this is the first report to identify *in vivo* associations between α4β2-nAChR availability, especially within basal forebrain, fronto-temporo-parietal cortices, and parahippocampus and episodic memory in patients with mild Alzheimer's dementia.

There is a strong association (significant following correction for multiple comparisons) between altered executive function/working memory and lower α4β2-nAChR availability, within the *a priori* defined fronto-parietal cortices in Alzheimer's dementia. Further, results of *post hoc* exploratory SPM analysis suggest, however not significant following testing for multiple comparisons, that there might be an additional relationship between executive function/working memory and lower α4β2-nAChR availability with the temporal cortex. Findings of two α4β2-nAChR PET/SPECT studies in mild-to-moderate Alzheimer's dementia using 2-^{18}F-F-A85380 or 5-^{123}I-I-A85380 demonstrated associations between impaired executive function and lower α4β2-nAChR availability, especially within the frontal cortex, supporting our results in part (Colloby *et al.*, 2010; Okada *et al.*, 2013). Thus, findings suggest that the *a priori* defined network comprised of the fronto-parietal cortices, being assumed to be mainly associated with executive function/working memory, might be extended to the temporal cortex if confirmed by future PET investigations (Levin *et al.*, 2006; Graef *et al.*, 2011; Ballinger *et al.*, 2016; Bettcher *et al.*, 2016).

There is no significant correlation between impaired attention and decreased α4β2-nAChR availability within the *a priori* selected brain regions, such as the frontal and parietal cortices using volume of interest analysis in Alzheimer's dementia. Exploratory SPM analysis suggests that, although not significant following correction for multiple comparisons, there may be a relationship between reduced α4β2-nAChR availability in frontal white matter and subcortical brain regions such as the thalamus and putamen and dysfunction of attention. The PET findings support the view that fronto-thalamic-striatal α4β2-nAChRs contribute to the functional cholinergic network of attention (Sarter *et al.*, 2001; Howe *et al.*, 2010).

Exploratory SPM analysis suggests that there might be a relationship between dysfunction of language and lower α4β2-nAChR availability within the right cerebellar cortex (crus 1 and 2) in Alzheimer's dementia. Although not significant following correction for multiple comparisons, this finding is in agreement with results of a meta-analysis investigating the functional topography of the cerebellum and identifying lobule VI and VII and crus 1 within the right posterior cerebellum to be associated with language (Stoodley and Schmahmann, 2009; Buckner, 2013). There is no significant relationship between visuospatial dysfunction and regional α4β2-nAChR availability in Alzheimer's dementia, which is in line with findings of prior α4β2-nAChR PET/SPECT studies (Meyer *et al.*, 2014).

In both study cohorts, there were no associations between education or age and α4β2-nAChR availability, and no sex-related differences of the α4β2-nAChR availability. Although previously reported using α4β2-nAChR PET/SPECT, the lack of a relationship between age or sex and α4β2-nAChR binding in this PET study may be explained by the relatively small size of the study cohorts, the small age range in both cohorts, and by the fact that in Alzheimer's dementia, α4β2-nAChR availability is influenced by distinct neuropathology (Meyer *et al.*, 2009; Mitsis *et al.*, 2009*a*).

There are the following limitations. First, the clinical diagnostic criteria of Alzheimer's dementia (NINCDS-ADRDA),

as used in this study, may lack accuracy. Enrichment of the Alzheimer's dementia group by biomarkers of amyloid pathology, like amyloid-β PET, was not approved by the regulatory authorities. Thus, our Alzheimer's dementia cohort might contain patients suffering from other forms of dementia. To reduce this risk, we investigated K_1 PET data within fronto-temporo-parietal cortices as calculated by pharmacokinetic modelling from the (−)-^{18}F-flubatine PET data. K_1 of (−)-^{18}F-flubatine is closely correlated to cerebral blood flow and may therefore serve as an indirect measure of the degree of neurodegeneration. Further, VBM analyses of grey matter density within the basal forebrain and hippocampus were carried out in Alzheimer's dementia and healthy controls. In Alzheimer's dementia, the K_1 PET and VBM analyses concordantly showed signs of neurodegeneration in brain regions typically affected in Alzheimer's dementia, by that supporting the clinical diagnoses. Second, although we investigated only mild Alzheimer's dementia, atrophy-related partial volume effects affecting α4β2-nAChR PET data analysis may be present and should be taken into account. To minimize atrophy-related effects, irregular brain tissue-containing volumes of interest were defined based on the individual MRI after MRI/PET co-registration. Additionally, grey matter density mask-weighted V_T values and partial volume effect corrected V_T values were calculated for each subject. The pattern of regionally lower V_TGMDW, V_TPVEC and V_T in Alzheimer's dementia compared with healthy controls, was similar. Furthermore, for those PET parameters very close correlations between V_T, V_TGMDW, and V_TPVEC and specific cognitive partial functions were found in Alzheimer's dementia. Therefore, a major effect of brain atrophy on these PET findings can be ruled out.

To summarize, in mild Alzheimer's dementia, there is a widespread reduction of cholinergic α4β2-nAChR availability especially within the hippocampus, fronto-temporal cortices, and basal forebrain, most pronounced within the mesial temporal cortex (hippocampus) and basal forebrain. Further, in Alzheimer's dementia, there is a relationship between networks of decreased α4β2-nAChR availability, especially within fronto-temporo-parietal cortices and basal forebrain and impairment of episodic memory, and within fronto-parietal cortices and impairment of executive function/working memory. This shows the potential of (−)-^{18}F-flubatine as PET biomarker of cholinergic α4β2-nAChR vulnerability and specific cognitive decline. Thus, (−)-^{18}F-flubatine might become a biomarker of progression of α4β2-nAChR neurodegeneration in Alzheimer's dementia. This hypothesis, however, needs to be proved by prospective, longitudinal PET investigations.

Acknowledgements

We thank all patients and healthy controls who participated in this study. We thank the PET technologists, PET radiochemists, cyclotron operators, and study coordinators of the Leipzig University Department of Nuclear Medicine for their skilful support.

Funding

The study was supported by a BMBF grant (Federal Ministry for Education and Research; no. 01EZ0820-3). S.G. received funding from the International Max Planck Research School on Neuroscience of Communication (IMPRS NeuroCom).

Supplementary material

Supplementary material is available at *Brain* online.

References

Aizenstein HJ, Nebes RD, Saxton JA, Price JC, Mathis CA, Tsopelas ND, et al. Frequent amyloid deposition without significant cognitive impairment among the elderly. Arch Neurol 2008; 65: 1509–17.

Ashburner J. A fast diffeomorphic image registration algorithm. Neuroimage 2007; 38: 95–113.

Ballinger EC, Ananth M, Talmage DA, Role LW. Basal forebrain cholinergic circuits and signaling in cognition and cognitive decline. Neuron 2016; 91: 1199–218.

Barthel H, Seibyl J, Sabri O. The role of positron emission tomography imaging in understanding Alzheimer's disease. Expert Rev Neurother 2015; 15: 395–406.

Benjamini Y, Hochberg Y. Controlling the false discovery rate: a practical and powerful approach to multiple testing. J R Stat Soc Series B Methodol 1995; 57: 289–300.

Bettcher BM, Mungas D, Patel N, Elofson J, Dutt S, Wynn M, et al. Neuroanatomical substrates of executive functions: beyond prefrontal structures. Neuropsychologia 2016; 85: 100–9.

Bohnen NI, Kaufer DI, Ivanco LS, Lopresti B, Koeppe RA, Davis JG, et al. Cortical cholinergic function is more severely affected in parkinsonian dementia than in Alzheimer disease: an in vivo positron emission tomographic study. Arch Neurol 2003; 60: 1745–8.

Brody AL, Mandelkern MA, London ED, Olmstead RE, Farahi J, Scheibal D, et al. Cigarette smoking saturates brain alpha 4 beta 2 nicotinic acetylcholine receptors. Arch Gen Psychiatry 2006; 63: 907–15.

Brust P, Patt JT, Deuther-Conrad W, Becker G, Patt M, Schildan A, et al. *In vivo* measurement of nicotinic acetylcholine receptors with ^{18}F-norchloro-fluoro-homoepibatidine. Synapse 2008; 62: 205–18.

Buchert R, Thomasius R, Wilke F, Petersen K, Nebeling B, Obrocki J, et al. A voxel-based PET investigation of the long-term effects of "Ecstasy" consumption on brain serotonin transporters. Am J Psychiatry 2004; 161: 1181–9.

Buckner RL. The cerebellum and cognitive function: 25 years of insight from anatomy and neuroimaging. Neuron 2013; 80: 807–15.

Cabeza R, Nyberg L. Imaging cognition II: an empirical review of 275 PET and fMRI studies. J Cogn Neurosci 2000; 12: 1–47.

Colloby SJ, Perry EK, Pakrasi S, Pimlott SL, Wyper DJ, McKeith IG, et al. Nicotinic ^{123}I-5IA-85380 single photon emission computed tomography as a predictor of cognitive progression in Alzheimer's disease and dementia with Lewy bodies. Am J Ger Psychiatry 2010; 18: 86–90.

Dani JA, Bertrand D. Nicotinic acetylcholine receptors and nicotinic cholinergic mechanisms of the central nervous system. Annu Rev Pharmacol Toxicol 2007; 47: 699–729.

Eickhoff S, Stephan KE, Mohlberg H, Grefkes C, Fink GR, Amunts K, et al. A new SPM toolbox for combining probabilistic cytoarchitectonic maps and functional imaging data. Neuroimage 2005; 25: 1325–35.

Ellis JR, Villemagne VL, Nathan PJ, Mulligan RS, Gong SJ, Chan JG, et al. Relationship between nicotinic receptors and cognitive function in early Alzheimer's disease: a 2-^{18}F-fluoro-A-85380 PET study. Neurobiol Learn Mem 2008; 90: 404–12.

Fazekas F, Chawluk JB, Alavi A, Hurtig HI, Zimmerman RA. MR signal abnormalities at 1.5 T in Alzheimer's dementia and normal aging. AJR Am J Roentgenol 1987; 149: 351–6.

Foxe D, Leyton CE, Hodges JR, Burrell JR, Irish M, Piguet O. The neural correlates of auditory and visuospatial span in logopenic progressive aphasia and Alzheimer's disease. Cortex 2016; 83: 39–50.

Francis PT, Palmer AM, Snape M, Wilcock GK. The cholinergic hypothesis of Alzheimer's disease: a review of progress. J Neurol Neurosurg Psychiatry 1999; 66: 137–47.

Friston KJ, Holmes A, Poline JB, Price CJ, Frith CD. Detecting activations in PET and fMRI: levels of inference and power. Neuroimage 1996; 40: 223–35.

Garibotto V, Tettamanti M, Marcone A, Florea I, Panzacchi A, Moresco R, et al. Cholinergic activity correlates with reserve proxies in Alzheimer's disease. Neurobiol Aging 2013; 34: 2694.e13–18. doi: 10.1016/j.neurobiolaging.2013.05.020. Epub 2013 Jun 29.

Gatterer, G. AKT Alters-Konzentrations-test. 2nd edn. Göttingen: Hogrefe Verlag GmbH & Co. KG; 2008.

Graef S, Schönknecht P, Sabri O, Hegerl U. Cholinergic receptor subtypes and their role in cognition, emotion, and vigilance control: an overview of preclinical and clinical findings. Psychopharmacology 2011; 215: 205–29.

Härting C, Markowitsch HJ, Neufeld H, Calabrese P, Deisinger K, Kessler J, eds. WMS-R Wechsler Gedächtnistest—revidierte fassung. 2nd edn. Bern; Göttingen; Toronto; Seattle: Verlag Hans Huber; 2000.

Hillmer AT, Wooten DW, Moirano JM, Slesarev M, Barnhart TE, Engle JW, et al. Specific α4β2 nicotinic acetylcholine receptor binding of F-18-nifene in the rhesus monkey. Synapse 2011; 65: 1309–18.

Howe WM, Ji J, Parikh V, Williams S, Mocaër E, Trocmé-Thibierge C, et al. Enhancement of attentional performance by selective stimulation of alpha4beta2(*) nAChRs: underlying cholinergic mechanisms. Neuropsychopharmacology 2010; 35: 1391–401.

Innis RB, Cunningham VJ, Delforge J, Fujita M, Gjedde A, Gunn RN, et al. Consensus nomenclature for in vivo imaging of reversibly binding radioligands. J Cereb Blood Flow Metab 2007; 27: 1533–9.

Kamkwalala AR, Newhouse PA. Beyond acetylcholinesterase inhibitors: novel cholinergic treatments for Alzheimer's disease. Curr Alzheimer Res 2017; 14: 377–92.

Kantarci K, Senjem ML, Lowe VJ, Wiste HJ, Weigand SD, Kemp BJ, et al. Effects of age on the glucose metabolic changes in mild cognitive impairment. AJNR Am J Neuroradiol 2010; 31: 1247–53.

Kendziorra K, Wolf H, Meyer PM, Barthel H, Hesse S, Becker GA, et al. Decreased cerebral α4β2 nicotinic acetylcholine receptor availability in patients with mild cognitive impairment and Alzheimer's disease assessed with positron emission tomography. Eur J Nucl Med Mol Imaging 2011; 38: 515–25.

Kim EJ, Cho SS, Jeong Y, Park KC, Kang SJ, Kang E, et al. Glucose metabolism in early onset versus late onset Alzheimer's disease: an SPM analysis of 120 patients. Brain 2005; 128: 1790–801.

Kimes AS, Horti AG, London ED, Chefer SI, Contoreggi C, Ernst M, et al. 2-^{18}F-F-A85380: PET imaging of brain nicotinic acetylcholine receptors and whole body distribution in humans. FASEB J 2003; 17: 1331–3.

Klingner M, Apelt J, Kumar A, Sorger D, Sabri O, Steinbach J, et al. Alterations in cholinergic and non-cholinergic neurotransmitter receptor densities in transgenic Tg2576 mouse brain with beta-amyloid plaque pathology. Int J Dev Neurosci 2003; 21: 57–69.

Kuhl DE, Minoshima S, Fessler JA, Frey KA, Foster NL, Ficaro EP, et al. In vivo mapping of cholinergic terminals in normal aging, Alzheimer's disease, and Parkinson's disease. Ann Neurol 1996; 40: 399–410.

Lehrl S. Mehrfachwahl-wortschatz-intelligenztest MWT-B. 5. unveränderte Aufl. Balingen: Spitta Verlag; 2005.

Lesné S, Koh MT, Kotilinek L, Kayed R, Glabe CG, Yang A, et al. A specific amyloid-beta protein assembly in the brain impairs memory. Nature 2006; 440: 352–7.

Levin ED, McClernon FJ, Rezvani AH. Nicotinic effects on cognitive function: behavioral characterization, pharmacological specification, and anatomic localization. Psychopharmacology 2006; 184: 523–39.

Lombardo S, Maskos U. Role of the nicotinic acetylcholine receptor in Alzheimer's disease pathology and treatment. Neuropharmacology 2015; 96: 255–62.

McKhann GM, Knopman DS, Chertkow H, Hyman BT, Jack CR Jr, Kawas CH, et al. The diagnosis of dementia due to Alzheimer's disease: recommendations from the National Institute on Aging-Alzheimer's Association workgroups on diagnostic guidelines for Alzheimer's disease. Alzheimers Dement 2011; 7: 263–9.

Meyer PM, Strecker K, Kendziorra K, Becker G, Hesse S, Woelpl D, et al. Reduced alpha4beta2*-nicotinic acetylcholine receptor binding and its relationship to mild cognitive and depressive symptoms in Parkinson disease. Arch Gen Psychiatry 2009; 66: 866–77.

Meyer PM, Tiepolt S, Barthel H, Hesse S, Sabri O. Radioligand imaging of α4β2* nicotinic acetylcholine receptors in Alzheimer's disease and Parkinson's disease. Q J Nucl Med Mol Imaging 2014; 58: 376–86.

Mitsis EM, Cosgrove KP, Staley JK, Bois F, Frohlich EB, Tamagnan GD, et al. Age-related decline in nicotinic receptor availability with (123)I-5-IA-85380 SPECT. Neurobiol Aging 2009a; 30: 1490–7.

Mitsis EM, Reech KM, Bois F, Tamagnan GD, Macavoy MG, Seibyl JP, et al. 123I-5-IA-85380 SPECT imaging of nicotinic receptors in Alzheimer disease and mild cognitive impairment. J Nucl Med 2009b; 50: 1455–63.

Morris JC, Heyman A, Mohs RC, Hughes JP, van Belle G, Fillenbaum G, et al. The Consortium to Establish a Registry for Alzheimer's Disease (CERAD). Part I. Clinical and neuropsychological assessment of Alzheimer's disease. Neurology 1989; 39: 1159–65.

Nees F. The nicotinic cholinergic system function in the human brain. Neuropharmacology 2015; 96: 289–301.

O'Brien JT, Colloby SJ, Pakrasi S, Perry EK, Pimlott SL, Wyper DJ, et al. Alpha4beta2 nicotinic receptor status in Alzheimer's disease using 123I-5IA-85380 single-photon-emission computed tomography. J Neurol Neurosurg Psychiatry 2007; 78: 356–62.

Okada H, Ouchi Y, Ogawa M, Futatsubashi M, Saito Y, Yoshikawa E, et al. Alterations in α4β2 nicotinic receptors in cognitive decline in Alzheimer's aetiopathology. Brain 2013; 136: 3004–17.

Patt M, Becker GA, Grossmann U, Habermann B, Schildan A, Wilke S, et al. Evaluation of metabolism, plasma protein binding and other biological parameters after administration of (−)-(18)F-Flubatine in humans. Nucl Med Biol 2014; 41: 489–94.

Patt M, Schildan A, Habermann B, Fischer S, Hiller A, Deuther-Conrad W, et al. Fully automated radiosynthesis of both enantiomers of ^{18}F-Flubatine under GMP conditions for human application. Appl Radiat Isot 2013; 80: 7–11.

Perry EK, Morris CM, Court JA, Cheng A, Fairbairn AF, McKeith IG, et al. Alteration in nicotine binding sites in Parkinson's disease, Lewy body dementia and Alzheimer's disease: possible index of early neuropathology. Neuroscience 1995; 64: 385–95.

Perry EK, Smith CJ, Perry RH, Whitford C, Johnson M, Birdsall NJ. Regional distribution of muscarinic and nicotinic cholinergic receptor binding activities in the human brain. J Chem Neuroanat 1989; 2: 189–99.

Pini L, Pievani M, Bocchetta M, Altomare D, Bosco P, Cavedo E, et al. Brain atrophy in Alzheimer's disease and aging. Ageing Res Rev 2016; 30: 25–48.

Richter N, Beckers N, Onur OA, Dietlein M, Tittgemeyer M, Kracht L, et al. Effect of cholinergic treatment depends on cholinergic integrity in early Alzheimer's disease. Brain 2018; 126: 903–15.

Rinne JO, Myllykylä T, Lönnberg P, Marjamäki P. A postmortem study of brain nicotinic receptors in Parkinson's and Alzheimer's disease. Brain Res 1991; 547: 167–70.

Rowe CC, Ellis KA, Rimajova M, Bourgeat P, Pike KE, Jones G, et al. Amyloid imaging results from the Australian Imaging, Biomarkers and Lifestyle (AIBL) study of aging. Neurobiol Aging 2010; 31: 1275–83.

Sabri O, Becker GA, Meyer PM, Hesse S, Wilke S, Graef S, et al. First-in-human PET quantification study of cerebral α4β2* nicotinic acetylcholine receptors using the novel specific radioligand (−)-(18)F-Flubatine. Neuroimage 2015; 118: 199–208.

Sabri O, Kendziorra K, Wolf H, Gertz HJ, Brust P. Acetylcholine receptors in dementia and mild cognitive impairment. Eur J Nucl Med Mol Imaging 2008; 35 (Suppl 1): S30–45.

Sarter M, Givens B, Bruno JP. The cognitive neuroscience of sustained attention: where top-down meets bottom-up. Brain Res Brain Res Rev 2001; 35: 146–60.

Sattler B, Kranz M, Starke A, Wilke S, Donat CK, Deuther-Conrad W, et al. Internal dose assessment of (−)-^{18}F-flubatine, comparing animal model datasets of mice and piglets with first-in-human results. J Nucl Med 2014; 55: 1885–92.

Scheltens P, Leys D, Barkhof F, Huglo D, Weinstein HC, Vermersch P, et al. Atrophy of medial temporal lobes on MRI in "probable" Alzheimer's disease and normal ageing: diagnostic value and neuropsychological correlates. J Neurol Neurosurg Psychiatry 1992; 55: 967–72.

Schliebs R, Arendt T. The cholinergic system in aging and neuronal degeneration. Behav Brain Res 2011; 221: 555–63.

Stoodley CJ, Schmahmann JD. Functional topography in the human cerebellum: a meta-analysis of neuroimaging studies. Neuroimage 2009; 44: 489–501.

Sunderland T, Hill JL, Mellow AM, Lawlor BA, Gundersheimer J, Newhouse PA, et al. Clock drawing in Alzheimer's disease. A novel measure of dementia severity. J Am Geriatr Soc 1989; 37: 725–9.

Teipel SJ, Sabri O, Grothe M, Barthel H, Prvulovic D, Buerger K, et al. Perspectives for multimodal neurochemical and imaging biomarkers in Alzheimer's disease. J Alzheimers Dis 2013; 33 (Suppl 1): S329–47.

Theofilas P, Ehrenberg AJ, Dunlop S, Di Lorenzo Alho AT, Nguy A, Leite RE, et al. Locus coeruleus volume and cell population changes during Alzheimer's disease progression: a stereological study in human postmortem brains with potential implication for early-stage biomarker discovery. Alzheimers Dement 2017; 13: 236–46.

Thomas BA, Cuplov V, Bousse A, Mendes A, Thielemans K, Hutton BF, et al. PETPVC: a toolbox for performing partial volume correction techniques in positron emission tomography. Phys Med Biol 2016; 61: 7975–93.

Thomas BA, Erlandsson K, Modat M, Thurfjell L, Vandenberghe R, Ourselin S, et al. The importance of appropriate partial volume correction for PET quantification in Alzheimer's disease. Eur J Nucl Med Mol Imaging 2011; 38: 1104–19.

Wong DF, Kuwabara H, Kim J, Brasic JR, Chamroonrat W, Gao Y, et al. PET imaging of high-affinity α4β2 nicotinic acetylcholine receptors in humans with ^{18}F-AZAN, a radioligand with optimal brain kinetics. J Nucl Med 2013; 54: 1308–14.

Yesavage JA, Brink TL, Rose TL, Lum O, Huang V, Adey M, et al. Development and validation of a geriatric depression screening scale: a preliminary report. J Psychiatr Res 1982-1983; 17: 37–49.

Yin Y, Wang Y, Gao D, Ye J, Wang X, Fang L, et al. Accumulation of human full-length tau induces degradation of nicotinic acetylcholine receptor α4 via activating calpain-2. Sci Rep 2016; 6: 27283. doi: 10.1038/srep27283.

Zaborszky L, Hoemke L, Mohlberg H, Schleicher A, Amunts K, Zilles K. Stereotaxic probabilistic maps of the magnocellular cell groups in human basal forebrain. Neuroimage 2008; 42: 1127–41.